Plasmon-Induced Transparency in Metamaterials

Shuang Zhang, Dentcho A. Genov, Yuan Wang, Ming Liu, and Xiang Zhang*

Nanoscale Science and Engineering Center, University of California, 5130 Etcheverry Hall, Berkeley, California 94720-1740, USA

(Received 19 December 2007; revised manuscript received 14 May 2008; published 23 July 2008)

A plasmonic ''molecule'' consisting of a radiative element coupled with a subradiant (dark) element is theoretically investigated. The plasmonic molecule shows electromagnetic response that closely resembles the electromagnetically induced transparency in an atomic system. Because of its subwavelength dimension, this electromagnetically induced transparency-like molecule can be used as a building block to construct a ''slow light'' plasmonic metamaterial.

DOI: 10.1103/PhysRevLett.101.047401 PACS numbers: 78.20.Ci, 42.25.Bs, 78.67.Pt

The localized surface plasmon has received much attention due to the interesting physics and important applications such as fluorescence resonance energy transfer and enhanced Raman scatterings [1,2]. The interaction between two or more plasmonic particles gives rise to interesting hybridization of the plasmonic modes, which can be utilized to tune the resonance frequency of the system [3]. Recently, the merging of plasmonics and metamaterials areas has led to the achievement of magnetic and negative index metamaterials in the optical frequencies, which may open up a new perspective towards achieving ultimate control of light in the nanoscale dimension [4–6].

A plasmonic mode can be either superradiant (radiative mode) or subradiant (dark mode) depending on how strong an incident light from free space can be coupled into the plasmonic mode [7]. The radiative mode has a large scattering cross section and a low quality factor due to the radiation coupling. On the contrary, the dark mode normally has a significantly larger quality factor, which is limited only by the loss of the metal. Naturally, this leads to the analogy of the dark mode with a metastable level in an atomic system. The metastable energy level is necessary for the realization of an electromagnetically induced transparency (EIT) medium [8–10]. For instance, in a three-level atomic EIT system, the coupling between an energy level ($|2\rangle$) with a dipole-allowed transition to the ground state ($|1\rangle$) and a metastable level ($|3\rangle$) by a pumping beam leads to a destructive interference between two pathways, namely, $|1\rangle - |2\rangle$ and $|1\rangle - |2\rangle - |3\rangle - |2\rangle$ [11]. This destructive interference results in a narrow transparent window within a broader absorption band. Recently, analogs of the EIT system using coupled microsize optical resonators have been proposed [12–18], which bring the original quantum phenomena into the realm of classical optics. In order to achieve the ultimate goal of a nanosized active optical circuit with switching and modulation capabilities, and in the pursuit of effective media exhibiting EIT-like optical properties, ''light slowing'' elements with deep subwavelength features are highly desired. In this Letter, we propose a coupled radiative-dark plasmonic mechanism to mimic the functionality of an atomic EIT system. This new approach is then used to construct the first EIT-like optical metamaterial consisting of coupled nanoscale plasmonic resonators. The plasmonic metamaterial has well-defined EIT-like effective properties and opens up the possibilities to construct devices of various scales and shapes while maintaining consistent optical properties that do not depend on the dimensions of the device. They can be designed for applications in either free space optics or an integrated optical circuit and, in particular, for slow light and enhanced nonlinear effects [19,20]. Additionally, it is interesting to note that the metamaterial approach toward EIT presented in this work and the recent theoretical propositions of using atomic EIT processes to achieve negative index materials [21,22] are examples how the development in one field inspires the other.

We begin by introducing a general description of an EIT-like plasmonic ''molecule.'' The molecule consists of two artificial ''atoms,'' a radiative plasmonic state $|a\rangle = \tilde{a}(\omega)e^{i\omega t}$, which strongly couples with the incident field $E_0 = \tilde{E}_0 e^{i\omega t}$, and a dark plasmonic state $|b\rangle = \tilde{b}(\omega)e^{i\omega t}$, which weakly couples to the incident light; both have a resonant frequency ω_0. For frequency close to the resonance $\delta = \omega - \omega_0 \ll \omega_0$, and assuming that the damping factors of the two resonators satisfy $\gamma_b \ll \gamma_a \ll \omega_0$, the field amplitude of both states (elements) can be described as linearly coupled Lorentzian oscillators

$$\begin{pmatrix} \tilde{a} \\ \tilde{b} \end{pmatrix} = -\begin{pmatrix} \delta + i\gamma_a & \kappa \\ \kappa & \delta + i\gamma_b \end{pmatrix}^{-1} \begin{pmatrix} g\tilde{E}_0 \\ 0 \end{pmatrix}, \quad (1)$$

where κ is the coupling between the two atoms and g is a geometric parameter indicating how strong the radiative mode (element) couples with the incident electromagnetic wave. In Eq. (1), we have assumed the dark plasmonic atom does not couple with the incident light. The amplitude of the dipole response of the radiative atom is given as

$$\tilde{a} = \frac{-g\tilde{E}_0(\delta + i\gamma_b)}{(\delta + i\gamma_a)(\delta + i\gamma_b) - \kappa^2}. \quad (2)$$

A short inspection of the above expression shows that the polarizability of the molecule, which is proportional to the amplitude $\tilde{a}$ of the radiative atom, has a very similar form as that in the EIT atomic system, especially in the case of zero detuning of the coupling laser frequency from

the corresponding atomic transition [11]. Provided the plasmonic molecule is much smaller than the wavelength of light, an effective medium can be constructed by these building blocks. The susceptibility of such an effective medium is proportional to the amplitude $\tilde{a}$, and assuming a small detuning $\delta \ll \{\gamma_a, \gamma_b, \kappa\}$, to the second-order approximation we can write

$$\chi = \chi_r + i\chi_i \sim \delta \frac{\kappa^2 - \gamma_b^2}{(\kappa^2 + \gamma_a\gamma_b)^2} + i\frac{\gamma_b}{\kappa^2 + \gamma_a\gamma_b} + iO(\delta^2). \tag{3}$$

The real part of the susceptibility disappears at transparency frequency (zero detuning). Since the second-order derivative of χ_r is zero, there is no dispersion in group velocity, and a pulse centered at the transparency frequency will travel through the medium without distortion. In the ideal case of $\gamma_b = 0$, the imaginary part of the susceptibility disappears, leading to an optically transparent effective medium. From Eq. (3), the slope of the real parts of susceptibility is inversely proportional to κ^2; e.g., a smaller coupling coefficient will result in a slower group velocity. On the other hand, in the realistic case of a finite γ_b, κ^2 needs to be sufficiently large to keep χ_i close to zero. Thus, there is a trade-off between a small loss and a large dispersion, which needs to be carefully balanced in the design of the EIT-like plasmonic elements.

Based on the above considerations, we turn to a specific design of a nanoplasmonic molecule for the realization of the EIT-like system. First we recognize that a simple metal strip may function as an optical dipole antenna [23] and thus could serve as the radiative or "bright atom" in the EIT-like plasmonic system. The resonance frequency of the metal strip can be readily tuned by varying its spatial dimension. Figure 1(a) shows the electric field amplitude versus frequency calculated near one of the metal strip ends. The numerical calculation is carried out using the commercial finite difference time domain (FDTD) software package (CST Microwave Studio), and silver is selected as a material due to low intrinsic loss [24]. For the chosen geometry, the resonance frequency is around 429 THz ($\lambda = 699$ nm, more than 5 times the antenna length), with a quality factor $Q \approx 11.8$, estimated from the linewidth of the resonance peak. The quality factor is mainly limited by the radiation dissipation, which comprises a large part of the total loss.

The dark atom consists of two parallel metal strips with a small separation, as shown in Fig. 1(b). This configuration has symmetric and antisymmetric modes, whose resonances are separated in the frequency domain. The antisymmetric mode has counterpropagating currents on the two strips; therefore, there is no direct electrical dipole coupling with the radiation wave, and it can be considered as a dark mode with a significantly longer dephasing time. We note that this parallel-metal-strip configuration has served as an artificial magnetic dipole in the optical frequencies [6]. The antisymmetric resonance frequency of

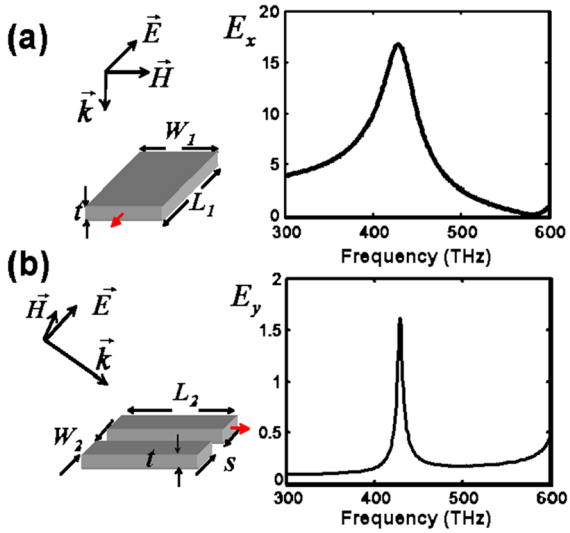

FIG. 1 (color online). (a) Left: The schematic of a silver optical antenna which functions as a radiative atom. The geometric parameters W_1, L_1, and t are 50, 128, and 20 nm, respectively. A plane wave is incident along the z direction, with $\vec{E}$ and $\vec{H}$ along the x and y directions. Right: The spectral response of an E_x probe (red arrow) placed 10 nm from the center of the end facet of the antenna. (b) Left: The schematic of a pair of metal strips forming a dark plasmonic atom. The geometric parameters W_2, L_2, and s are 30, 100, and 30 nm, respectively. The incident wave vector lies in the y-z plane and is tilted 45° from the z direction, with the electric field along the x direction (perpendicular to the metal strips). Right: The spectral response of an E_y probe (red arrow) placed 10 nm from the center of the end facet of one of the metal strips in the dark atom.

the dark atom is designed to coincide with that of the radiative atom [see Fig. 1(b)], thus being consistent with the general model described before. The quality factor of the dark atom is $Q \approx 82$, which is about 1 order of magnitude larger than that of the radiative atom. The quality factor of the dark atom is limited by the metal loss, which may be improved by incorporating gain medium.

In contrast to an atomic EIT system, where the coupling between two energy levels is realized with a pump beam, the coupling between the radiative and dark atoms in the plasmonic EIT system is determined by their spatial separation [Fig. 2(a)]. Figure 2(b) shows both real and imaginary parts of the electric field probed at the end of the radiative metal strip [red arrow in Fig. 2(a)] for different separations between the radiative and dark atoms. Note that the field is the sum of the incident light and the dipole response of the radiative atom; as a result, it is linearly related to the dipole polarizability. Thus, by investigating the field response, we can gain insight into the effective susceptibility of the system. For all separations, the coupling between the radiative and dark atoms leads to a narrow dip at the center of the broad peak for the imaginary part of electric field, which confirms the EIT-like destructive interference between the two pathways: direct dipole excitation of the radiative atom from the incident wave and

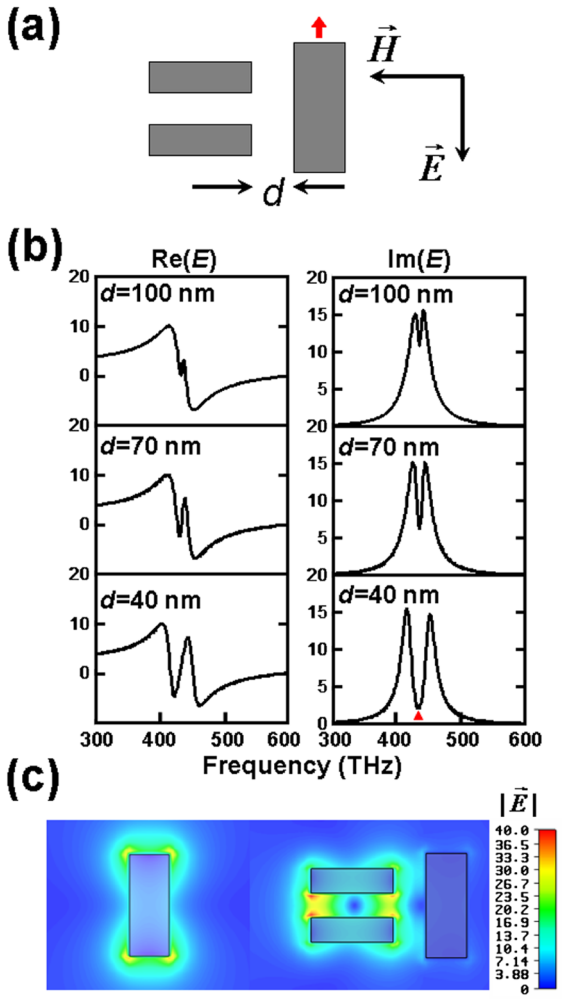

FIG. 2 (color online). (a) Top view of the plasmonic system consisting of a radiative element and a dark element with a separation d, with light incident at the normal direction. (b) The real part and imaginary part of a E_x probe placed at 10 nm from the end facet of the radiative antenna red arrow in (a) for separations ranging from 40 to 100 nm between the radiative and dark elements. (c) The 2D field plot of an uncoupled radiative atom (left) and a radiative atom coupled with a dark atom with a separation of 40 nm (right) at a frequency of 428.4 THz, as indicated by the red triangle in (b).

excitation of the dark atom (by the radiative atom) coupling back to the radiative atom. At a large separation of 100 nm, where the coupling is weak, the contrast of the dip is very small, which is due to the finite quality factor of the resonance in the dark atom. With the increase of coupling (decreasing separation), the dip widens and becomes deeper, similar to the quantum EIT in an atomic system. At the frequency corresponding to the transparency (dip in the imaginary part of the field), the real part of the electric field shows a highly dispersive behavior, indicating that a light pulse travels at a significantly lower group velocity in a metamaterial consisting of this coupled plasmonic system. To visualize this destructive interference between the two pathways, we compare the 2D distribution of an electric field at 428.4 THz for the radiative antenna uncoupled [Fig. 2(c), left] and coupled with the dark atom [Fig. 2(c), right]. Without coupling to the dark atom, the radiative antenna is strongly excited by the incident plane wave with a high electric field forming at its end facets. By placing the dark atom 40 nm from the radiative one, the electromagnetic field is coupled back and forth between the radiative and dark atoms, leading to a destructive interference and a suppressed state in the radiative atom with a much weaker electric field at its ends.

Next, we consider an optical EIT-like metamaterial with the coupled radiative-dark molecule as its building blocks [Fig. 3(a)]. In the following discussion, the separation

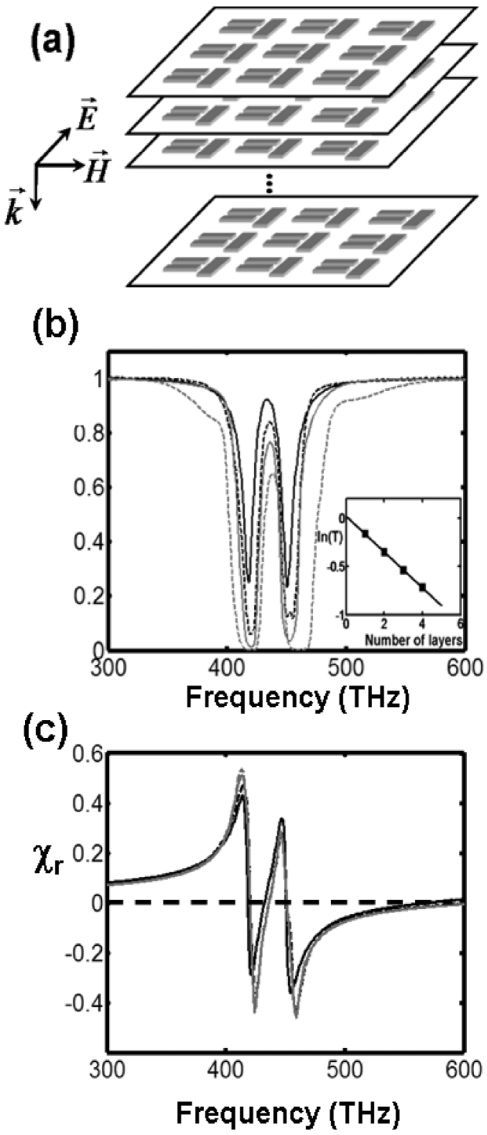

FIG. 3. (a) The schematic of a plasmonic EIT metamaterial. The transmission spectra (b) and the real part of the susceptibility (c) for one (black curve), two (black dashed curve), three (gray curve), and four (gray dashed curve) layers of metamaterial. The inset in (b) shows the natural logarithm of peak transmission vs the number of layers along the propagation direction at the transparency frequency.

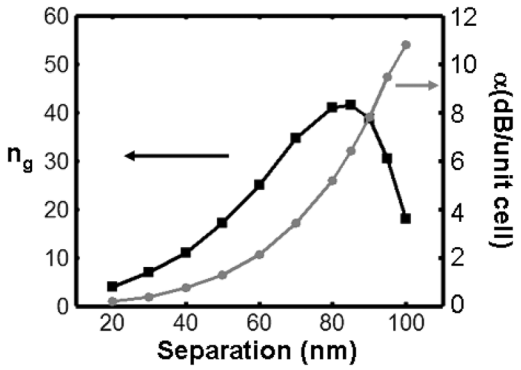

FIG. 4. The dependence of the group refractive index (black curve) and propagating loss (gray curve) at the transparency frequency on the separation between the radiative and dark atoms.

between the dark and radiative atoms is fixed at 40 nm, with all other parameters kept the same as before. The plasmonic molecules are arranged periodically with a spacing of 400 nm in the x-y plane and a spacing of 200 nm in the z (propagation) direction. Figure 3(b) shows the transmission for metamaterials consisting of one to four layers of unit cells along the propagation direction. In the figures, the transmission exhibits a peak within a broader absorption band, which is similar to the transmission usually observed in an atomic EIT system. With the increase of the unit cells along the propagation, the transparent peak decreases due to loss in the metal. As presented in the inset in Fig. 3(b), a linear relation between the natural logarithm of peak transmission versus number of layers is observed, indicating that a single propagating mode dominates for light traversing through the metamaterial. From the slope we calculate the imaginary part of susceptibility to be 0.052. The real parts of the susceptibility for all of the different numbers of unit cells are derived from the transmission phase shifts and shown in Fig. 3(c). The calculated susceptibilities are almost the same regardless of the number of unit cells along the propagation, suggesting that the structure functions as a true optical effective medium. The group refractive index is estimated from the slope of χ_r at the transparency frequency, which is about 10.9. In the FDTD simulations, the mesh size of the spatial discretization is 4 nm in the metal and 8 nm in the surrounding air. Further refining of the mesh size (1.5 nm in the metal and 3 nm in air) leads to a relative change of the group refractive index by less than 3%.

Figure 4 shows the dependence of the group refractive index and loss of the EIT metamaterials on the separation distance between the artificial radiative and dark atoms. In correspondence with the general model, for strong coupling $\kappa \gg \sqrt{\gamma_a \gamma_b}$, we have $\chi_r \sim 1/\kappa^2$ and an increase in the group index is observed for increased separation (or decreased coupling). This trend persists up to $d = 85$ nm, where a maximum group index of 41 is achieved, which corresponds roughly to the condition $\kappa(d) = \sqrt{\gamma_a \gamma_b}$ according to Eq. (3). On the other hand, the loss of the EIT material increases dramatically with decreasing coupling (or increasing separation). The intrinsic loss of the plasmonic EIT metamaterial could be lowered by incorporating gain medium or operation at low temperatures [25–27]. Furthermore, we note that, while we focused only on a specific EIT-like metamaterial in the optical frequency, the general principle can be readily extended to longer wavelengths such as terahertz and microwave frequencies, where the dissipative loss in the metamaterial is lower.

In summary, we have demonstrated a novel plasmonic metamaterial which closely mimics the EIT phenomena in an atomic system. Although the slowdown factor (~10) is much lower than the EIT in an atomic system, it has advantages such as room temperature operation, wide bandwidth, and, more importantly, ready integration with a nanoplasmonic circuit.

This work was supported by AFOSR MURI (Grant No. 50432), SINAM, and NSEC under Grant No. DMI-0327077.

*Corresponding author.
xiang@berkeley.edu

[1] T. Ha *et al.*, Proc. Natl. Acad. Sci. U.S.A. **93**, 6264 (1996).
[2] S. M. Nie and S. R. Emery, Science **275**, 1102 (1997).
[3] E. Prodan *et al.*, Science **302**, 419 (2003).
[4] S. Linden *et al.*, Science **306**, 1351 (2004).
[5] S. Zhang *et al.*, Phys. Rev. Lett. **95**, 137404 (2005).
[6] V. M. Shalaev *et al.*, Opt. Lett. **30**, 3356 (2005).
[7] M. I. Stockman, S. V. Faleev, and D. J. Bergman, Phys. Rev. Lett. **87**, 167401 (2001).
[8] S. E. Harris, Phys. Today **50**, No. 7, 36 (1997).
[9] K. J. Boller, A. Imamoglu, and S. E. Harris, Phys. Rev. Lett. **66**, 2593 (1991).
[10] D. F. Phillips *et al.*, Phys. Rev. Lett. **86**, 783 (2001).
[11] M. Fleischhauer, A. Imamoglu, and J. P. Marangos, Rev. Mod. Phys. **77**, 633 (2005).
[12] L. Maleki *et al.*, Opt. Lett. **29**, 626 (2004).
[13] D. D. Smith *et al.*, Phys. Rev. A **69**, 063804 (2004).
[14] M. F. Yanik *et al.*, Phys. Rev. Lett. **93**, 233903 (2004).
[15] Q. F. Xu *et al.*, Phys. Rev. Lett. **96**, 123901 (2006).
[16] K. Totsuka, N. Kobayashi, and M. Tomita, Phys. Rev. Lett. **98**, 213904 (2007).
[17] A. G. Litvak and M. D. Tokman, Phys. Rev. Lett. **88**, 095003 (2002).
[18] G. Shvets and J. S. Wurtele, Phys. Rev. Lett. **89**, 115003 (2002).
[19] D. Budker *et al.*, Phys. Rev. Lett. **83**, 1767 (1999).
[20] C. Liu *et al.*, Nature (London) **409**, 490 (2001).
[21] J. Kastel *et al.*, Phys. Rev. Lett. **99**, 073602 (2007).
[22] C. M. Krowne, Phys. Lett. A **372**, 3926 (2008).
[23] L. Novotny, Phys. Rev. Lett. **98**, 266802 (2007).
[24] M. A. Ordal, Appl. Opt. **22**, 1099 (1983).
[25] J. Seidel, S. Grafström, and L. Eng, Phys. Rev. Lett. **94**, 177401 (2005).
[26] M. A. Noginov *et al.*, Opt. Lett. **31**, 3022 (2006).
[27] M. T. Hill *et al.*, Nat. Photon. **1**, 589 (2007).